

# Noise Characteristics of Charge Tunneling *via* Localized States in Metal–Molecule–Metal Junctions

Youngsang Kim,<sup>†,‡,§</sup> Hyunwook Song,<sup>\*,§</sup> Dongwoo Kim,<sup>†</sup> Takhee Lee,<sup>\*,\*</sup> and Heejun Jeong<sup>†,\*</sup>

<sup>†</sup>Department of Applied Physics, Hanyang University, Ansan 426-791, Korea, and <sup>‡</sup>Department of Nanobio Materials and Electronics, and Department of Materials Science and Engineering, Gwangju Institute of Science and Technology, Gwangju 500-712, Korea. <sup>§</sup>These authors contributed equally to this work. <sup>‡</sup>Present address: Department of Physics, University of Konstanz, 78457 Konstanz, Germany.

**ABSTRACT** We report the noise characteristics of charge transport through an alkyl-based metal–molecule–metal junction. Measurements of the  $1/f$  noise, random telegraph noise, and shot noise demonstrated the existence of localized traps in the molecular junctions. These three noise measurements exhibited results consistent with trap-mediated tunneling activated over  $\sim 0.4$  V by trapping and detrapping processes *via* localized states (or defects). The noise characterizations will be useful in evaluating the influences of localized states on charge transport in molecular or other electronic junctions.

**KEYWORDS:** molecular junctions · localized states ·  $1/f$  noise · random telegraph noise · shot noise

When the feature size of an active component of an electronic device shrinks to the molecular scale, it is expected that the device characteristics will become more vulnerable to fluctuations or noise in the molecular system, owing to imperfections in the molecular layers on both the metallic electrodes and the metal–molecule interfaces.<sup>1,2</sup> Although significant progress has been made in investigating the charge transport characteristics of metal–molecule–metal junctions,<sup>3–5</sup> there have been very few studies on the noise characteristics of molecular systems.<sup>6,7</sup> Current noise has a universal role in the charge transport and defect characterization of electronic systems. Thus, noise measurements can provide important insights into charge transport through metal–molecule–metal junctions, particularly regarding localized states in the molecular tunnel barriers, which are very difficult to examine by conventional current–voltage measurements.<sup>8</sup>

Here, we report a detailed study on the noise characterization of metal–molecule–metal junctions. Specifically, we examined  $1/f$  noise (at low frequency), random tele-

graph noise (RTN), and shot noise (at high frequency) characteristics using an alkyl-based molecular junction, demonstrating the effect of localized states on charge transport through molecular junctions. In this study, the main emphasis is on the verification of defective molecular junctions by examination of the consistent features from the results of the three noise types based on the existence of the localized states at room temperature.

## RESULTS AND DISCUSSION

Figure 1a illustrates a device structure in which 1,6-hexanedithiol [SH-(CH<sub>2</sub>)<sub>6</sub>-SH, denoted as HDT] molecules self-assembled between two gold electrodes to form metal–molecule–metal junctions.<sup>9</sup> The junction diameter was estimated to be  $\sim 100$  nm from a scanning electron microscopy image as shown in Figure 1b (see Methods). We have investigated 16 devices containing localized states, among  $\sim 400$  devices which were estimated as well-defined metal–molecule–metal junctions. We note that the probability ( $16/400 = 4\%$ ) to observe such defective metal–molecule–metal junction devices is well consistent with the previous results obtained from temperature–variable current–voltage measurements.<sup>9</sup> Figure 1c schematically illustrates the details of the measurement setup. We used a ground-isolated 16-bit analog-digital converter (ADC) to detect the RTN. A battery-powered low-noise current amplifier (Ithaco 1211) was used for all measurements. Low frequency current noise and shot noise were measured using a spectrum analyzer (Stanford Research SR780). The instrumental

\*Address correspondence to hjeong@hanyang.ac.kr, tlee@gist.ac.kr.

Received for review February 7, 2010 and accepted July 27, 2010.

Published online August 2, 2010. 10.1021/nn100255b

© 2010 American Chemical Society

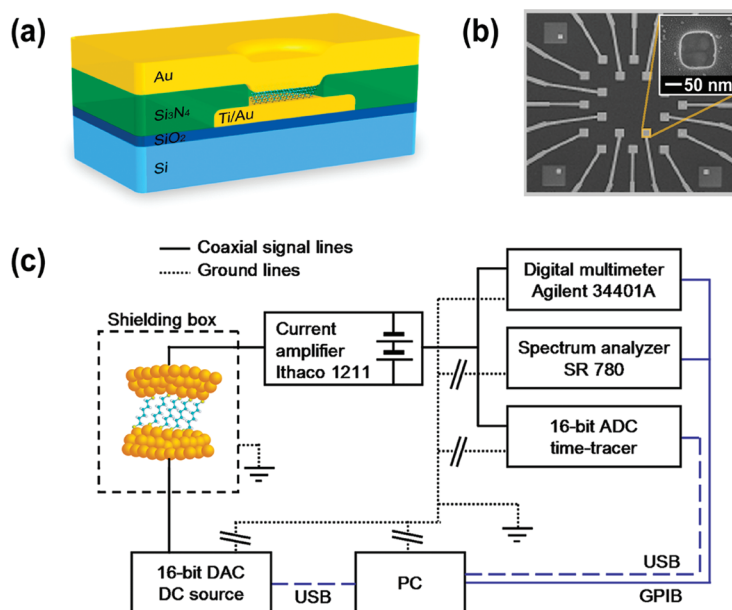


Figure 1. (a) Schematic diagram of the molecular device structure with a molecular structure of hexanedithiol. (b) Magnified image of an array of 20 bottom electrodes. The inset shows a nanowell with a junction diameter of 100 nm, made by electron-beam lithography. Prior to deposit of the common top electrode (not shown here), self-assembled monolayers are formed into the nanowells. (c) Schematic picture of the measurement setup. All the grounds of the system are isolated to remove ground-loops (tilted double-lines), and the device is filtered against RF interference by using shielding. The connections between PC and instruments are made with GPIB cables (blue solid line) while the connections between PC and AD/DAC are USB cable (blue dashed line).

setup was calibrated prior to the noise measurement by measuring the equilibrium Johnson–Nyquist voltage noise,  $S_V = 4k_BRT$ , as a function of temperature  $T$ , where  $k_B$  is the Boltzmann constant and  $R$  is the sample resistance.<sup>10,11</sup>

The low frequency current noise power spectrum of the Au–HDT–Au junction at different voltages (from 0.2 to 1.0 V) is shown in Figure 2. Low frequency  $1/f$  noise measurement is a powerful tool for characterizing defects in electronic devices.<sup>12</sup> All of the spectra follow a  $1/f$  (up to  $\sim 20$  Hz) or  $1/f^2$  (above  $\sim 20$  Hz) power law depending on the frequency, which indicates a superposition of  $1/f$  and generation-recombination (GR) noise (Lorentzian distribution), as follows:<sup>11,13</sup>

$$S(f) = \frac{A}{f^\alpha} + \sum_i \frac{B_i}{1 + (f/f_{0i})^2}, \quad \text{where } f_{0i} = \frac{1}{2\pi\tau_i} \quad (1)$$

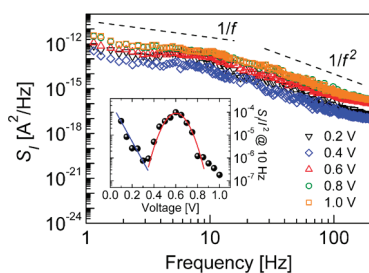
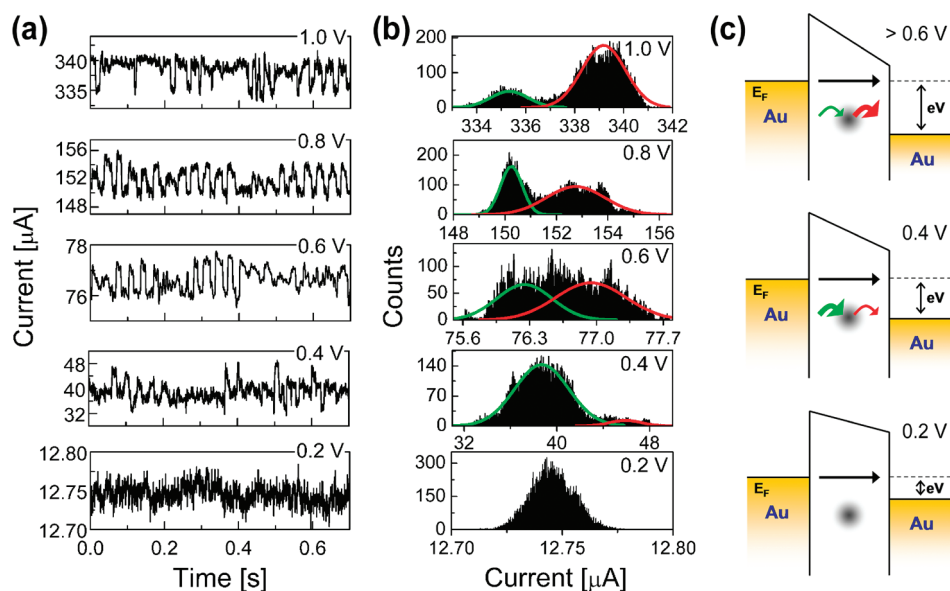


Figure 2. Low frequency power spectrum current noise of Au–HDT–Au junction. Inset shows the voltage dependence of the normalized power spectrum current noise at frequency  $f = 10$  Hz, indicating a localization of defects.

$A$  is the amplitude of the  $1/f$  noise,  $B_i$  is the amplitude of the GR noise caused by defects,  $f_{0i}$  is the cutoff frequency of the GR noise, and  $\tau_i$  is the lifetime of the carriers. The Lorentzian distribution in the low frequency noise spectra results from the processes of trapping/detrapping of charge carriers into/from localized states in the molecular junction.<sup>14</sup> The voltage dependence of the normalized current noise power spectrum ( $S_I/I^2$ ) at a frequency of 10 Hz is shown in the inset of Figure 2. The normalized noise spectra display exponential decreases below  $\sim 0.4$  V (blue lines), whereas local increases, fit to a Gaussian distribution (red lines), are observed in the bias range  $V \geq \sim 0.4$  V. More similar noise characteristics measured from other devices are presented in the Supporting Information (Figure S2). These local Gaussian-shaped bumps from the low frequency current noise can be explained by a model of a two-level tunneling system, such as asymmetric double-barrier tunneling.<sup>7</sup> The local Gaussian-shaped bumps occur due to the localization of defects; if the defects are distributed uniformly, the normalized power spectrum will be distributed linearly without showing a local bump (see Figure S3 in the Supporting Information).<sup>7,15,16</sup>

We also measured time-dependent current fluctuations, referred to as random telegraph noise (RTN). Measuring RTN enables the investigation of traps in nanoscale devices.<sup>13,17,18</sup> In Figure 3a, current traces were recorded for 0.7 s at room temperature as a function of the applied voltage, and the corresponding histograms of the current fluctuation data are plotted in Fig-



**Figure 3.** (a) Time-dependent two-level RTNs of Au–HDT–Au junction. RTNs were recorded at 21875 points at a sampling rate of  $3 \mu\text{s}/\text{point}$  at room temperature for 0.7 s. (b) Corresponding histograms for the RTNs. The histograms are fitted with Gaussian peaks where green and red lines indicate trapping and detrapping events, respectively. (c) Schematic energy band diagrams of the molecular junction with a single localized trap.

ure 3b. We observed a discrete temporal fluctuation, stochastically caused by the trapping and detrapping process of some charges within a bunch of charges *via* localized states; the down state (low-current level) corresponds to trapping, and the up state (high-current level) corresponds to detrapping. In Figure 3b, the histograms were fit to Gaussian functions, where green and red lines indicate trapping and detrapping events, respectively. We found that the two-level current fluctuation appears at  $V \geq \sim 0.4$  V. Figure 3c illustrates the energy band structure of a molecular junction with a localized trap, at different applied voltages. At 0.4 V, the trapping events prevail, which can result from the charging effect on a localized state in the molecular barrier. By contrast, the detrapping process became predominant with increasing bias (above 0.6 V), which implies that the large potential difference can lead to re-emission of the trapped charge carriers. Other RTN data which do not contain the localized states are presented in the Supporting Information (Figure S3).

Furthermore, we performed frequency-independent shot noise measurements to probe the existence of the localized states in the molecular junction. The shot noise is the result of current fluctuations induced by the discrete charges, and is highly dependent on the correlations between the tunneling charges in the molecular junction.<sup>6,8</sup> The processes of charge trapping and detrapping *via* localized states play an important role in shot noise because a trapped carrier can behave like a fixed charge, and this trapped carrier thus significantly influences the correlations among the charge carriers flowing through the molecular junction. The shot noise characteristics can be described in terms of the Fano factor ( $F$ ), defined as  $F =$

$S_I/2eI/|\coth(eV/2k_B T)|$ .<sup>6,19</sup> In the absence of a correlation between tunneling charges (see Supporting Information), the Fano factor would indicate full shot noise,  $F = 1$ , and super-Poissonian shot noise,  $F > 1$ , is associated with a correlation between tunneling charges resulting from Coulomb repulsion and scattering.<sup>8,20</sup>

Figure 4 shows the results of shot noise measurement for Au–HDT–Au junctions. The Fano factor indicates full shot noise ( $F = 1$ ) in the low bias region below  $\sim 0.4$  V, indicating uncorrelated transport, and at  $\sim 0.4$  V it increases to super-Poissonian shot noise ( $F > 1$ ). Such shot noise enhancement can be understood as follows. If there are a few localized states (two or more) within the molecular junction, the Coulomb energy,  $U \sim e^2/(4\pi\epsilon_r\epsilon_0 r)$ , between the localized states becomes high enough to detect the fluctuations at room temperature, where  $r$  is the distance between the localized states,  $\epsilon_r$  is the relative permittivity of alkanethiol monolayers,<sup>21,22</sup> and  $\epsilon_0$  is the permittivity of free space. In this molecular system, charge carriers can tunnel through the molecular barrier without correlations when the localized states are not activated in the mo-

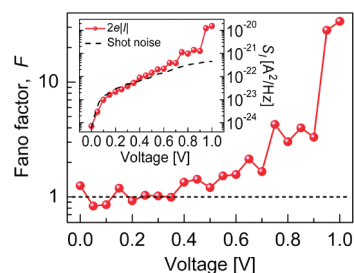


**Figure 4.** The Fano factor ( $F$ ) as a function of the applied voltage. The super-Poissonian shot noise ( $F > 1$ ) is observed at  $V \geq 0.4$  V. Inset shows the plot of the measured shot noise and  $2eI$  as a function of the applied voltage.

lecular junction, in the low bias region below  $\sim 0.4$  V, thus exhibiting full shot noise ( $F = 1$ ). However, when a localized state starts to be charged at  $\sim 0.4$  V, other energy levels of localized states can be shifted by Coulomb interaction between the localized states. If the deformed energy of localized states approaches the Fermi level, it is discharged and the current increases *via* the localized states nearly aligned to the Fermi level as quasi-resonance. As a result, the fluctuation is increased and the shot noise is enhanced to super-Poissonian shot noise ( $F > 1$ ).<sup>23–25</sup>

From the three different noise measurements, we consistently observed the existence of localized states in the molecular nanowell junctions. The localized states can be formed by defects that may be unintentionally

introduced into the molecular layer in the junction or the metal–molecule interfaces. Alternatively, the penetration of gold particles during the metallization process for the top electrode may also be the origin of the localized states.<sup>26,27</sup>

## CONCLUSIONS

We have performed a series of noise characterizations of  $1/f$ , RTN and shot noise in alkyl-based molecular junctions. Strong evidence for the existence of localized states (or defects) was observed as charge fluctuations in these measurements of noise. Noise measurements can be a useful tool for inspecting defect-mediated transport in molecular-scale electronic devices.

## METHODS

**Device Fabrication.** The detail fabrication is as following. The bottom electrodes (5 nm Ti/50 nm Au) are deposited using an electron beam evaporator on a silicon wafer with a 500 nm thick layer of SiO<sub>2</sub> by standard photolithography and lift-off process. The bottom electrodes are arrayed in the center of the device structure connected with probe contact pads in the outer sides, as shown in Figure 1b. A 50 nm thick Si<sub>3</sub>N<sub>4</sub> film was then deposited using plasma-enhanced chemical vapor deposition (PECVD) on the silicon wafer that had the prepatterned bottom electrodes for device isolation. Then electron-beam lithography and reactive ion etching (RIE) process were used to form nanowell structures through the Si<sub>3</sub>N<sub>4</sub> layer.<sup>28</sup> After cleaning with piranha solution (30% hydrogen peroxide added to 66% sulfuric acid in a ratio of 1:3), we immersed the wafer into a solution of alkanethiol (from Sigma-Aldrich) to assemble the 1,6-hexanedithiol (HDT) [HS(CH<sub>2</sub>)<sub>6</sub>SH] monolayer on the exposed Au surface of the bottom electrode. For molecular deposition, a 5 mM solution of alkanethiol was prepared in 10 mL of ethanol. The deposition was done on Au surface in solution for 1–2 days inside a nitrogen-filled glovebox with an oxygen level less than 10 ppm to avoid unintentional incorporation of impurities in the devices. Each sample was then rinsed with a few milliliters of ethanol and gently blown dry in a stream of nitrogen to remove noncovalently attached alkanethiol molecules on the Au surface. As the last step, the common top electrode (50-nm-thick Au) was deposited using a shadow mask.<sup>29–32</sup>

**Acknowledgment.** This work was supported by the Korea Science and Engineering Foundation (KOSEF) (Grant No. 2009-0075053) by the Korean Ministry of Education, Science and Technology (MEST). T.L. and H.S. would like to thank the National Research Laboratory (NRL) program by MEST.

**Supporting Information Available:** Images of fabricated devices, and more noise characteristics of metal–molecule–metal junctions which contain localized states as well as those which do not contain localized states. This material is available free of charge *via* the Internet at <http://pubs.acs.org>.

## REFERENCES AND NOTES

- Weiss, E. A.; Chiechi, R. C.; Kaufman, G. K.; Kriebel, J. K.; Li, Z.; Duati, M.; Rampi, M. A.; Whitesides, G. M. Influence of Defects on the Electrical Characteristics of Mercury-Drop Junctions: Self-Assembled Monolayers of *n*-Alkanethiols on Rough and Smooth Silver. *J. Am. Chem. Soc.* **2007**, *129*, 4336–4349.
- Love, J. C.; Estroff, L. A.; Kriebel, J. K.; Nuzzo, R. G.; Whitesides, G. M. Self-Assembled Monolayers of Thiolates on Metals as a Form of Nanotechnology. *Chem. Rev.* **2005**, *105*, 1103–1170.
- Nitzan, A.; Ratner, M. A. Electron Transport in Molecular Wire Junctions. *Science* **2003**, *300*, 1384–1389.
- Galperin, M.; Ratner, M. A.; Nitzan, A.; Troisi, A. Nuclear Coupling and Polarization in Molecular Transport Junctions: Beyond Tunneling to Function. *Science* **2008**, *319*, 1056–1060.
- Song, H.; Kim, Y.; Jang, Y. H.; Jeong, H.; Reed, M. A.; Lee, T. Observation of Molecular Orbital Gating. *Nature* **2009**, *462*, 1039–1043.
- Djukic, D.; van Ruitenbeek, J. M. Shot Noise Measurements on a Single Molecule. *Nano Lett.* **2006**, *6*, 789–793.
- Clément, N.; Pleutin, S.; Seitz, O.; Lenfant, S.; Vuillaume, D.  $1/f^{\gamma}$  Tunnel Current Noise through Si-Bound Alkyl Monolayers. *Phys. Rev. B* **2007**, *76*, 205407.
- Blanter, Y. M.; Büttiker, M. Shot Noise in Mesoscopic Conductors. *Phys. Rep.* **2000**, *336*, 1–166.
- Song, H.; Lee, T.; Choi, N. J.; Lee, H. A Statistical Method for Determining Intrinsic Electronic Transport Properties of Self-Assembled Alkanethiol Monolayer Devices. *Appl. Phys. Lett.* **2007**, *91*, 253116.
- Chen, C.-Y.; Kuan, C.-H. Design and Calibration of a Noise Measurement System. *IEEE Trans. Instrum. Meas.* **2000**, *49*, 77–82.
- Raoult, J.; Pascal, F.; Delseny, C.; Marin, M.; Deen, M. J. Impact of Carbon Concentration on  $1/f$  Noise and Random Telegraph Signal Noise in SiGe:C Heterojunction Bipolar Transistors. *J. Appl. Phys.* **2008**, *103*, 114508.
- Weissman, M. B.  $1/f$  Noise and Other Slow, Nonexponential Kinetics in Condensed Matter. *Rev. Mod. Phys.* **1998**, *60*, 537–571.
- Simon, A. B.; Paltiel, Y.; Jung, G.; Berger, V.; Schneider, H. Measurements of Non-Gaussian Noise in Quantum Wells. *Phys. Rev. B* **2007**, *76*, 235308.
- Ke, L.; Dolmanan, S. B.; Shen, L.; Vijila, C.; Chua, S. J.; Png, R.-Q.; Chia, P. J.; Chua, L.-L.; Ho, P. K.-H. Impact of Self-Assembled Monolayer on Low Frequency Noise of Organic Thin Film Transistors. *Appl. Phys. Lett.* **2008**, *93*, 153507.
- Rogers, C. T.; Buhman, R. A. Composition of  $1/f$  Noise in Metal–Insulator–Metal Tunnel Junctions. *Phys. Rev. Lett.* **1984**, *53*, 1272–1275.
- Carbone, A.; Kotowska, B. K.; Kotowski, D. Space-Charge-Limited Current Fluctuations in Organic Semiconductors. *Phys. Rev. Lett.* **2005**, *95*, 236601.
- Machlup, S. Noise in Semiconductors: Spectrum of a Two-Parameter Random Signal. *J. Appl. Phys.* **1954**, *25*, 341–343.
- Yuzhelevski, Y.; Yuzhelevski, M.; Jung, G. Random Telegraph Noise Analysis in Time Domain. *Rev. Sci. Instrum.* **2000**, *71*, 1681–1688.
- Sukhorukov, E. V.; Burkard, G.; Loss, D. Noise of a Quantum Dot System in the Cotunneling Regime. *Phys. Rev. B* **2001**, *63*, 125315.

20. Aleshkin, V. Y.; Reggiani, L.; Reklaitis, A. Electron Transport and Shot Noise in Ultrashort Single-Barrier Semiconductor Heterostructures. *Phys. Rev. B* **2001**, *63*, 085302.
21. Rampi, M. A.; Schueller, O. J. A.; Whitesides, G. M. Alkanethiol Self-Assembled Monolayers as the Dielectric of Capacitors with Nanoscale Thickness. *Appl. Phys. Lett.* **1998**, *72*, 1781–1783.
22. Sahalov, H.; O'Brien, B.; Stebe, K. J.; Hristova, K.; Searson, P. C. Influence of Applied Potential on the Impedance of Alkanethiol SAMs. *Langmuir* **2007**, *23*, 9681–9685.
23. Chen, Y.; Webb, R. A. Full Shot Noise in Mesoscopic Tunnel Barriers. *Phys. Rev. B* **2006**, *73*, 035424.
24. Savchenko, A. K.; Safonov, S. S.; Roshko, S. H.; Bagrets, D. A.; Jouravlev, O. N.; Nazarov, Y. V.; Linfield, E. H.; Ritchie, D. A. Shot Noise as a Probe of Electron Transport via Localised States in Sub-Micrometer Barriers. *Phys. Stat. Sol. (b)* **2005**, *242*, 1229–1232.
25. Safonov, S. S.; Savchenko, A. K.; Bagrets, D. A.; Jouravlev, O. N.; Nazarov, Y. V.; Linfield, E. H.; Ritchie, D. A. Enhanced Shot Noise in Resonant Tunneling via Interacting Localized States. *Phys. Rev. Lett.* **2003**, *91*, 136801.
26. Petta, J. R.; Slater, S. K.; Ralph, D. C. Spin-Dependent Transport in Molecular Tunnel Junctions. *Phys. Rev. Lett.* **2004**, *93*, 136601.
27. Yu, L. H.; Zangmeister, C. D.; Kushmerick, J. G. Origin of Discrepancies in Inelastic Electron Tunneling Spectra of Molecular Junctions. *Phys. Rev. Lett.* **2007**, *98*, 206803.
28. Amar, A.; Lozes, R. L.; Sasaki, Y.; Davis, J. C.; Packard, R. E. Fabrication of Submicron Apertures in Thin Membranes of Silicon Nitride. *J. Vac. Sci. Technol., B* **1993**, *11*, 259–262.
29. Seo, K.; Lee, H. Molecular Electron Transport Changes upon Structural Phase Transitions in Alkanethiol Molecular Junctions. *ACS Nano* **2009**, *3*, 2469–2476.
30. Lee, T.; Wang, W.; Klemic, J. F.; Zhang, J. J.; Su, J.; Reed, M. A. Comparison of Electronic Transport Characterization Methods for Alkanethiol Self-Assembled Monolayers. *J. Phys. Chem. B* **2004**, *108*, 8742–8750.
31. Wang, W.; Lee, T.; Reed, M. A. Mechanism of Electron Conduction in Self-Assembled Alkanethiol Monolayer Devices. *Phys. Rev. B* **2003**, *68*, 035416.
32. Song, H.; Lee, T.; Choi, N.-J.; Lee, H. Statistical Representation of Intrinsic Electronic Tunneling Characteristics through Alkyl Self-Assembled Monolayers in Nanowell Device Structures. *J. Vac. Sci. Technol., B* **2008**, *26*, 904–908.